PHYSICAL REVIEW A **79**, 060503(R) (2009)

# Separated oscillatory-field microwave measurement of the $2\,^3P_1-2\,^3P_2$ fine-structure interval of atomic helium

J. S. Borbely, M. C. George, L. D. Lombardi, M. Weel, D. W. Fitzakerley, and E. A. Hessels
*Department of Physics and Astronomy, York University, 4700 Keele Street, Toronto, Ontario, Canada M3J 1P3*
(Received 21 February 2009; published 30 June 2009)

The $2\,^3P_1-2\,^3P_2$ interval in helium is measured using microwave separated oscillatory fields. Our measured result is $2\,291\,177.53\pm0.35$ kHz . A disagreement with theory of over 15 kHz indicates a major problem with two-electron QED calculations. If this disagreement is resolved, measurements of both $2\,^3P$ fine-structure intervals at this accuracy would lead to a six-parts-per-billion determination of the fine-structure constant.

DOI: 10.1103/PhysRevA.79.060503 PACS number(s): 32.30.Bv, 06.20.Jr

The present work continues the long history of precision measurements of the $2\,^3P$ fine structure of helium [1–5]. The main goal of these measurements is to determine the fine-structure constant, $\alpha$, from the larger (29.6 GHz) $2\,^3P_1-2\,^3P_0$ interval with the smaller (2.3 GHz) $2\,^3P_1-2\,^3P_2$ interval testing the two-electron QED theoretical calculations necessary to determine $\alpha$. The present work differs by 36 standard deviations from theory [6,7]. If this discrepancy is resolved, measurements of both $2\,^3P$ fine-structure intervals at the current accuracy would determine $\alpha$ to 6 ppb. The most precise determination of $\alpha$ (0.37 ppb) is from the magnetic moment of the electron ($g_e$-2) [8]. Independent determinations of $\alpha$ [9] are needed to allow $g_e$-2 to test QED to 0.37 ppb (the most precise test of QED theory) and to search for physics beyond the standard model [8].

In this $2\,^3P$ measurement separated oscillatory fields (SOFs) are used, compared to previous measurements which used continuous fields for excitation [1–5]. SOFs allow for narrower linewidths (0.8–1.7 MHz) than the 3.25 MHz natural linewidth and also allow for a variety of line shapes. Figure 1 shows the experimental setup. A thermal beam of $2\,^3S_1$ metastable He is created in a dc discharge [3] and the $2\,^3S_1(m=0)$ state is depopulated by repeatedly driving $2\,^3S_1(m=0)-2\,^3P_0$ with a linearly polarized 1.08 $\mu$m diode laser (A in Fig. 1). $2\,^3S_1(m=\pm1)$ atoms are driven up to $2\,^3P_1(m=0)$ by a 15 ns laser pulse (B1 in Fig. 1, pulsed using two passes through an acousto-optic modulator), which is followed by the two 2.3 GHz SOF microwave pulses [P1 and P2 of Fig. 1(c), of duration $D=50$, 100, or 150 ns and separated in time by $T=300$, 400, 500, or 600 ns] which drive the $2\,^3P_1(m=0)-2\,^3P_2(m=0)$ transition. Atoms can decay to $2\,^3S_1(m=0)$ only if the microwave transition is driven since the $2\,^3P_1(m=0)-2\,^3S_1(m=0)$ branching ratio is zero. This $2\,^3S_1(m=0)$ population is excited to $2\,^3P_0$ with laser C and the resulting fluorescence is collected on a 77 K InGaAs photodiode.

The microwave transitions are driven inside of a 50 $\Omega$ coaxial transmission line [Fig. 1(a)]. To double the signal size, another laser beam (B2) repeats the experiment on the other side of the 50 $\Omega$ line [inset of Fig. 1(a)]. Microwaves (referenced to a Rb clock) are pulsed using fast switches and amplified to $P_\mu=25-125$ W by a solid-state amplifier. The relative phase of P1 and P2 is controlled by additional switches which direct the pulses through paths L1 or L2 that differ in length by a half wavelength ($\lambda_\mu/2$). Every 79 ms, the relative phase is toggled between 0° and 180° [using *a*, *b*, *c*, or *d* of Fig. 1(c)], and the difference in signal is recorded by a lock-in amplifier. The resulting signals as a function of microwave frequency ($f_\mu$) are shown in Fig. 2 for 3 of the 10 line shapes used. The SOF envelope has a width of $1/D$, the SOF interference has a width of $1/2T$, and the SOF signal decreases as $e^{-T/\tau}$, where $\tau=98$ ns is the $2\,^3P$ lifetime. The data of Fig. 2 are fit to the expected SOF line shape (solid line). Figure 2(d) shows residuals from one fit. For all 10 line shapes used, the residuals are very symmetric ($\chi^2_{reduced}<0.5$). The 477 data runs are taken with different experimental parameters, with each run including $\geq$20 repetitions of 3 s data points at 99 $f_\mu$s. Small line-shape distortions caused by the slightly different power through L1 and L2 cancel when averaging over *a*, *b*, *c*, and *d* of Fig. 1(c). This experiment was performed blind with the $f_\mu$ axis of Fig. 2 shifted by an unknown $\Delta f_\mu$ that was not revealed until 48 h prior to presenting this work.

The largest systematic correction is due to a dc magnetic field $\vec{B}=B_0\hat{z}$ applied to remove *m* state degeneracies. The $2\,^3P_1(m=0)-2\,^3P_2(m=0)$ transition has a small quadratic 0.5283 kHz/G$^2$ [10] second-order Zeeman shift. The Zeeman correction uncertainty is governed by the 1% uncertainty of $B_0$, which is measured using a Hall probe and using $2\,^3P$ $\Delta m=1$ linear Zeeman shifts. The data taken at 3 B

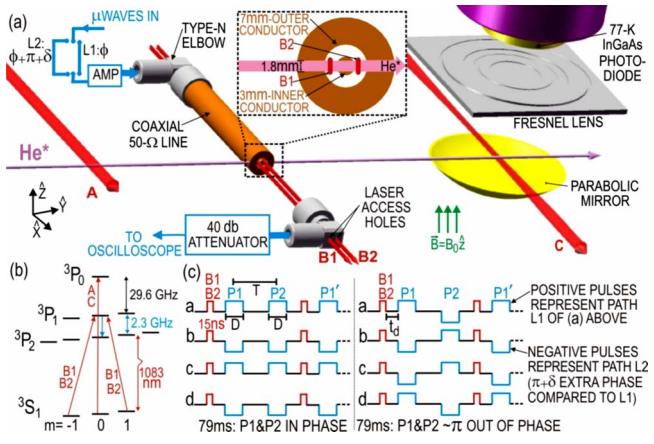


FIG. 1. (Color online) Schematic of the experiment with (a) an expanded cross-sectional view of the 50 $\Omega$ line, (b) energy-level diagram showing the transitions, and (c) timing diagram for four versions of the SOF measurement. See text for details.

 

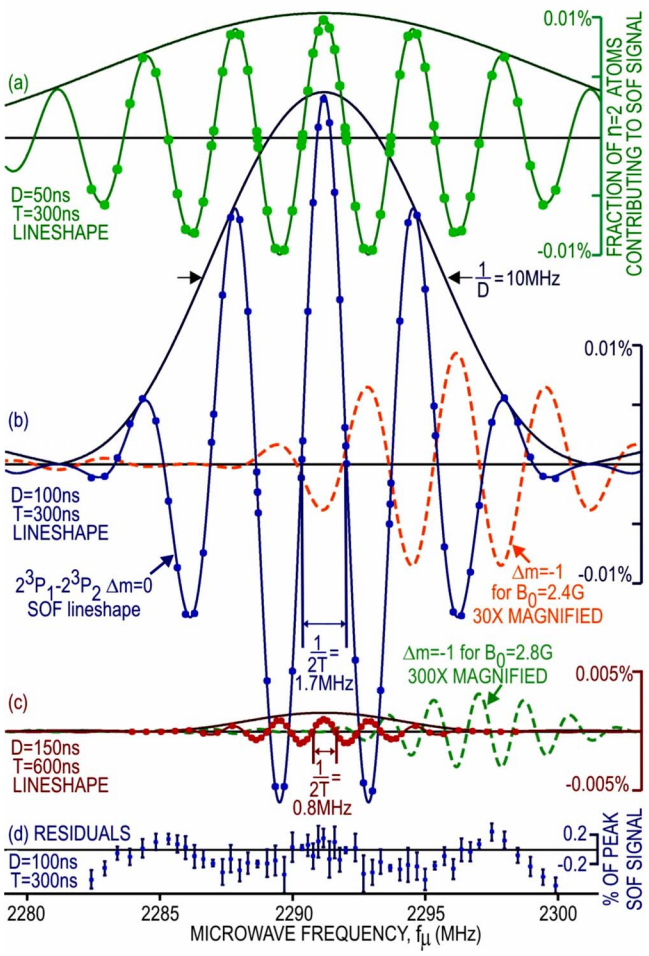


FIG. 2. (Color online) [(a)–(c)] Three of the ten line shapes used and (d) residuals. The uncertainties in (a)–(c) are five times smaller than the points and even smaller for repeated points near the zero crossings as shown by the smaller error bars in (d).

fields with shifts of 4–12 kHz (Table I) confirm that the corrections are well understood.

A concern is that a tiny fraction of the atoms are driven from $2\,^3P_1(m=0)$ to $2\,^3P_2(m=\pm 1)$ by small $B_y$ microwave fields which arise from the circular field lines inside the 50 Ω line. The expected $\Delta m=-1$ signal [see Fig. 2(b)] could shift the main $\Delta m=0$ SOF line shape. Fortunately, the $\Delta m=+1$ signal is expected to be of the same size but to the left of resonance. The symmetric residuals [such as Fig. 2(d)] give strong evidence that the $\Delta m=\pm 1$ signals occur symmetrically and therefore cause no shift. Even if a shift does occur, it is smaller for larger $D$ since there is less overlap of the $\Delta m=\pm 1$ signals, as shown by the dashed line in Fig. 2(c) and is smaller for larger $B_0$ since the $\Delta m=\pm 1$ signals Zeeman shift away from the $\Delta m=0$ resonance. The consistency of centers for different $B_0$ and $D$ indicates that any such effect is small. Furthermore, any shift would reverse when $\vec{B}$ is reversed from $\hat{z}$ to $-\hat{z}$, as is the case for half of the data.

A more subtle effect occurs if the polarization of lasers B1 and B2 is at an angle $\gamma \neq 0°$ from $\hat{y}$. B1 and B2 can then excite $2\,^3S_1(m=1)-2\,^3P_1(m=1)$ [or, similarly, $2\,^3S_1(m=-1)-2\,^3P_1(m=-1)$]. Imperfect microwave polarization can then drive these atoms from $2\,^3P_1(m=1)$ to $2\,^3P_2(m=0)$. The effect is small because it requires that both laser and microwave polarizations be imperfect. However, since the initial and final states are the same as for the intended transitions, there is a quantum-mechanical interference between the two ways of getting from $2\,^3S_1(m=1)$ to $2\,^3P_2(m=0)$. Resulting distortions of the line shapes are modeled and cause shifts which are zero if $\gamma=0°$ and grow linearly with $\gamma$. By minimizing the $2\,^3S_1(m=0)$ population when $P_\mu=0$, $\gamma$ is set to $<1°$. The value of $\gamma$ is confirmed by passing it through a carefully aligned Brewster plate. Some data taken with $\gamma=+10°$ or $-10°$ are shifted by $<1150$ Hz, and thus an uncertainty of 120 Hz is assigned to data for which $\gamma<1°$, as shown in Table I. This effect depends on the delay time $t_d$ between the laser pulse and P1 of Fig. 1(c) because the Zeeman shift of $2\,^3P_1(m=1)$ relative to $2\,^3P_2(m=0)$ causes these states to accumulate different phases ($e^{-iEt_d/\hbar}$). The consistency of line centers for $t_d=50$, 80, and 110 ns and for different $T$, $D$, and $B_0$ (where different shifts are expected) further confirms that this effect is small.

The key SOF parameter is the relative phase of P1 and P2 of Fig. 1(c). If L2 of Fig. 1(a) is not exactly $L1+\lambda_\mu/2$, this relative phase is $\pi+\delta$ and shifts the SOF center by $+\delta/4\pi T$ [for $a$ and $d$ of Fig. 1(c)] and $-\delta/4\pi T$ (for $b$ and $c$). The

TABLE I. Systematic corrections are each studied by varying at least one experimental parameter. The net correction is listed in the final column with one standard deviation uncertainties in the last digits in parentheses.

| Systematic effect | Parameter range | Shift (uncertainty) (in kHz) | | |
|---|---|---|---|---|
| | | Min. | Max. | Average |
| Zeeman shift | $B_0$: 3–5 G | −4.29(9) | −11.61(23) | −6.52(13) |
| Phase distortions | $D$: 50–150 ns | 0.23(15) | 1.07(48) | 0.59(18) |
| ac shifts | $P_\mu$: 25–125 W | −0.05(1) | −0.21(5) | −0.17(4) |
| Pressure shift | $P$: 2–20 μtorr | 0.00(9) | 0.00(91) | 0.00(9) |
| Light shift | $P_L$: 1.2–12 mW | 0.00(6) | 0.00(55) | 0.00(16) |
| Hole distortion | $T$: 300–600 ns | 0.00(2) | 0.00(19) | 0.00(4) |
| Polarization | $\gamma$: $<1$–$10°$ | 0.00(12) | 0.00(115) | 0.00(12) |

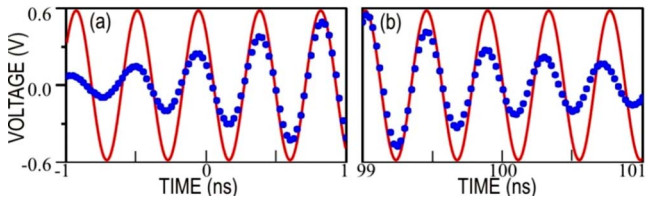


FIG. 3. (Color online) The beginning (a) and end (b) of a 100 ns microwave pulse. The voltage is recorded every 25 ps by a Tektronix DPO7354 oscilloscope. A sine wave is superimposed (solid curve) to help illustrate the phase distortions.

average of $a$ and $b$ and of $c$ and $d$ remains unshifted, and the $a$ minus $b$ and $c$ minus $d$ differences determine that $\delta = 0.31°$ for the L1 and L2 used here. The switches, amplifier, and other microwave components cause phase distortions of the microwave pulses as can be seen by an oscilloscope. Figure 3 shows two 2 ns slices of a single oscilloscope trace that are at the start and end of a 100 ns microwave pulse. A large phase shift can be seen at −0.7 and 100.7 ns. In addition, a slow 0.01 deg/ns phase progression occurs during the central portion (not shown in Fig. 3) of the pulse. Since both P1 and P2 experience these same phase distortions, there is no effect on their relative phase. However, some atoms decay out of the $2\,^3P$ state during P2 and therefore experience the full phase distortions of P1 but only part of the phase distortions of P2. Such atoms have a shift in their line center. To model this shift, the SOF experiment is simulated by numerically integrating Schrödinger's equation (including radiative decay to $2\,^3S$) using the microwave fields derived from the oscilloscope traces. The integrations use the fourth-order Runge-Kutta method with fifth-order polynomial interpolations between each of the 100 000 25-ps points in each of the oscilloscope traces obtained every 3 s over the 2500 h of atomic data collection. The integrations (performed using hundreds of processors) also include the motion of the atoms since the microwave fields depend on the position of the atom within the 50 Ω line. The simulated line shapes are almost identical to those of Fig. 2 but when fit, show small shifts due to the phase distortions. These shifts are applied to each individual data run and are summarized in Table I. The uncertainties in these corrections come from (1) a statistical uncertainty in the fits of the simulated line shapes (0.05 kHz), (2) an uncertainty in the oscilloscope time scale (0.09 kHz), and (3) a 25% uncertainty in how well the oscilloscope traces represent the microwave field seen by the atoms. The main concern for (3) is microwave reflections since the oscilloscope has a much larger reflection ($\Gamma = 0.28$) than any other microwave component. To test for reflected pulses that return to the oscilloscope (but are not seen by the atoms), a $\lambda_\mu/4$ long section, which reverses the sign of these reflected pulses, is sometimes added before the oscilloscope. To test for further effects, the numerical integrations are repeated using different initial positions for the atoms, speeds for the atoms, and normalizations of the oscilloscope traces. In all cases, the integrations give results that agree to 25% or better. Integrations that artificially eliminate the large phase distortions at the beginning and end of the pulses indicate the shifts are primarily due to the slow phase progression throughout the pulse, which has a smaller effect for shorter pulses, as shown in Table I. Phase distortion effects scale as $1/T$. The consistency of centers for different $T$ and $D$ confirms the validity of the applied phase distortion corrections.

Possible light shifts could result if the 15 ns laser pulse of Fig. 1(c) is not entirely extinguished before P1. Using a heterodyne technique, an extinction ratio of $>10^5$ is found. Light shifts could also result for the tiny fraction of $2\,^3P$ atoms which survive a time $2T+t_d$ and interact with a third microwave pulse, P1′ of Fig. 1(c). The SOF interference of P2 and P1′ is influenced by the laser pulse between them. The data taken at different laser powers are consistent with no light shifts and limit the shifts (on average) to $<50$ Hz/mW, as indicated in Table I.

The 1.8 mm circular hole of Fig. 1(a), which allows the He beam to pass through the inner and outer conductors of the 50 Ω line, distorts the microwave fields. These fields are modeled using the EMPIRE software package. The wave fronts are no longer planar near the holes, and therefore the relative phase of P1 and P2 seen by an atom depends on its speed and trajectory. Fortunately, the wave fronts are exactly planar at the central plane of the hole and the phase distortions along trajectories symmetric about this plane are equal and opposite. If the atomic trajectories are symmetric about the central plane, then shifts due to these phase distortions perfectly cancel. Even if the trajectories are not symmetric, the shifts still cancel when averaged over the equal quantities of data taken with microwaves traveling in the $\hat{x}$ and $-\hat{x}$ directions. To account for the unlikely possibility that a different set of trajectories contribute to the signal for the $\hat{x}$ and $-\hat{x}$ data, an uncertainty is included in Table I based on modeling using integrations of Schrödinger's equation with the EMPIRE fields. For larger $T$, the modeled effect increases as atoms travel further into the field distortions.

Small ac Stark shifts [11] result from the microwave electric field perturbing the $2\,^3P_1$ and $2\,^3P_2$ states via electric-dipole matrix elements connecting them to $n\,^3S$ and $n\,^3D$ states. Similar ac Zeeman shifts are a factor of 5 smaller and are due to the microwave magnetic field and magnetic-dipole matrix elements to other $2\,^3P_J$ states. These shifts are reduced by a factor of $D/T$ for SOF [11] since the atoms do not experience a microwave field during the time between the 2 pulses. The shifts increase linearly with $P_\mu$ from 25 to 125 W and are listed in Table I along with a 25% uncertainty due to the uncertainty in $P_\mu$. Possible pressure shifts are limited by the data collected at ten times higher vacuum pressure to be $<45$ Hz/$\mu$torr, as indicated in Table I. Care is taken to ensure that $P_\mu$ is independent of $f_\mu$. This independence is verified using oscilloscope traces and a precisely calibrated calorimeter [12]. Doppler shifts are small because of the slow thermal speed of the atoms (2100 m/s [3]) and because the microwaves travel perpendicular to the He beam. Even if this alignment is not perfect, the Doppler shifts for $\hat{x}$ and $-\hat{x}$ microwave propagation directions cancel.

Table II shows the final measured result for the $2\,^3P_1 - 2\,^3P_2$ interval and compares it to previous experiments and to theory. A $36\sigma$ discrepancy with theory is 2 orders of magnitude larger than expected for uncalculated $\alpha^6$ Rydberg terms [7], indicating an outstanding problem in two-electron QED theory. Smaller discrepancies (of 1.63, 3.53,

TABLE II. Recent experiment and theory of 2 $^3P$ He fine structure. Values are in MHz with one standard deviation uncertainties in the last digits in parentheses. Standard deviations from the present work are in square brackets.

| | $2\,^3P_1-2\,^3P_2$ | | $2\,^3P_1-2\,^3P_0$ |
|---|---|---|---|
| Present work | 2291.17753(35) | | |
| | Previous measurements | | |
| Shiner *et al.* [2] | 2291.1759(10) | [1.5$\sigma$] | |
| Hessels *et al.* [3] | 2291.1740(14) | [2.4$\sigma$] | 29616.9509(9) |
| Gabrielse *et al.* [4] | 2291.17559(51) | [3.1$\sigma$] | 29616.95166(70) |
| Inguscio *et al.* [5] | | | 29616.9527(10) |
| | Theory | | |
| Drake [6] | 2291.15462(31) | [49$\sigma$] | 29616.94642(18) |
| Pachucki [7] | 2291.16113(30) | [36$\sigma$] | 29616.94301(17) |

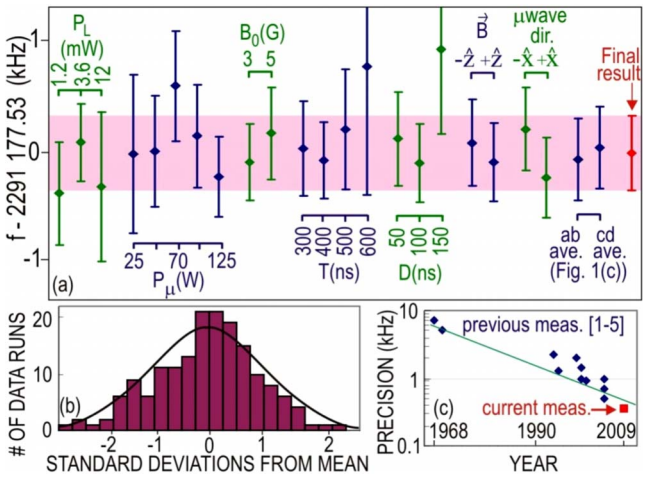


FIG. 4. (Color online) (a) Measured line centers show excellent agreement for various experimental parameters. (b) The statistical distribution of line centers about the final measured value. (c) The increasing precision of He 2 $^3P$ measurements.

and 1.94 kHz) appear between previous measurements and the present work. The strength of the present work is that the linewidth and line shape can be varied, whereas in previous measurements systematic effects could more easily be masked by a single line shape. No discrepancies appear between the large variation in experimental parameters and line shapes of the present measurement. Figure 4(a) shows the excellent agreement of the measured center for different $P_L$, $P_\mu$, $B_0$, $T$, $D$, directions of $\vec{B}$ and of microwave propagation, and SOF schemes of Fig. 1(c). The present 350 Hz uncertainty is dominated by the systematic effects of Table I. The statistical uncertainty is $<20$ Hz, with the vast majority of data used to study systematic effects. Figure 4(b) shows that the variation in line centers for the data runs have the expected normal distribution. The standard deviations of Fig. 4(b) are statistical uncertainties only, showing that the data runs are in excellent agreement even before systematic uncertainties are considered. Figure 4(c) illustrates that this SOF measurement continues the trend of increasingly precise measurements of the 2 $^3P$ intervals. Refinements are underway, and better control of all of the systematic effects seems possible, making a 100 Hz SOF measurement within reach. In particular, the $B$ field can be better measured, the laser polarizations better controlled, and better microwave components (or active feedback if necessary) can reduce the microwave phase distortions. The SOF method should apply equally well to the 29.6 GHz 2 $^3P$ interval although even more care will have to be taken to eliminate phase distortions. Once a 100 Hz measurement of the $2\,^3P_1-2\,^3P_0$ interval is made, a determination of $\alpha$ to 1.6 ppb is possible if sufficiently accurate theory becomes available.

*Note added*. Recently, Pachucki and Yerokhin [13] eliminated the discrepancy between experiment and theory for this interval.

This work was supported by NSERC, CRC, CFI, and OIT of Canada and the computations by SHARCNET.

[1] W. E. Lamb, Jr., Phys. Rev. **105**, 559 (1957); F. D. Colegrove *et al.*, Phys. Rev. Lett. **3**, 420 (1959); F. M. Pichanick, R. D. Swift, C. E. Johnson, and V. W. Hughes, Phys. Rev. **169**, 55 (1968); S. A. Lewis, F. M. Pichanick, and V. W. Hughes, Phys. Rev. A **2**, 86 (1970).

[2] D. Shiner, R. Dixson, and P. Zhao, Phys. Rev. Lett. **72**, 1802 (1994); J. Castillega, D. Livingston, A. Sanders, and D. Shiner, *ibid.* **84**, 4321 (2000).

[3] C. H. Storry and E. A. Hessels, Phys. Rev. A **58**, R8 (1998); C. H. Storry, M. C. George, and E. A. Hessels, Phys. Rev. Lett. **84**, 3274 (2000); M. C. George, L. D. Lombardi, and E. A. Hessels, *ibid.* **87**, 173002 (2001).

[4] T. Zelevinsky, D. Farkas, and G. Gabrielse, Phys. Rev. Lett. **95**, 203001 (2005).

[5] F. Minardi, G. Bianchini, P. C. Pastor, G. Giusfredi, F. S. Pavone, and M. Inguscio, Phys. Rev. Lett. **82**, 1112 (1999); G. Giusfredi *et al.*, Can. J. Phys. **83**, 301 (2005).

[6] G. W. F. Drake, Can. J. Phys. **80**, 1195 (2002).

[7] K. Pachucki, Phys. Rev. Lett. **97**, 013002 (2006).

[8] D. Hanneke, S. Fogwell, and G. Gabrielse, Phys. Rev. Lett. **100**, 120801 (2008).

[9] M. Cadoret *et al.*, Phys. Rev. Lett. **101**, 230801 (2008); V. Gerginov *et al.*, Phys. Rev. A **73**, 032504 (2006).

[10] Z. C. Yan and G. W. F. Drake, Phys. Rev. A **50**, R1980 (1994).

[11] S. R. Lundeen and F. M. Pipkin, Metrologia **22**, 9 (1986).

[12] R. F. Clark and A. Jurkus, Rev. Sci. Instrum. **39**, 660 (1968).

[13] K. Pachucki and V. A. Yerokhin, Phys. Rev. A **79**, 062516 (2009).